Carbohydrate Polymers 92 (2013) 2306–2313

Contents lists available at SciVerse ScienceDirect

Carbohydrate Polymers

journal homepage: www.elsevier.com/locate/carbpol

# Characterization of arenga starch in comparison with sago starch

Dede R. Adawiyah [a], Tomoko Sasaki [b], Kaoru Kohyama [b,*]

[a] Department of Food Science and Technology, Faculty of Agricultural Technology, Bogor Agricultural Technology, Bogor 16002, Indonesia
[b] National Food Research Institute, National Agriculture and Food Research Organization, 2-1-12 Kannondai, Tsukuba, Ibaraki 305-8642, Japan

ARTICLE INFO

*Article history:*
Received 3 April 2012
Received in revised form 4 December 2012
Accepted 7 December 2012
Available online 16 December 2012

*Keywords:*
Gelatinization
Swelling
Viscoelasticity
Texture

ABSTRACT

The aim of this research was to characterize the composition and physical properties of palm starch obtained from *Arenga pinnata* in comparison with another palm starch from *Metroxylon sago*. The amylose contents of both starches were not significantly different. Peak gelatinization temperature was also similar at approximately 67 °C, but arenga starch showed a narrower range of gelatinization temperature than sago. The crystallinity and swelling power capacity of arenga starch were lower than those of sago. Arenga and sago starch paste at low concentrations showed shear thinning behavior, and sago formed a more viscous sol/paste than arenga. The sol–gel transition concentration of sago starch paste was found at a lower concentration than arenga starch. At high concentrations, gel from arenga starch was more rigid than that of sago. The breaking properties and texture profile of both starch gels were also clearly different, suggesting that they are suited for different applications.



## 1. Introduction

Palm starch is an important source of starch in tropical countries. It is prepared from the pith of several genera of palms *Metroxylon* (species *Metroxylon sago*) and *Arenga* (species *Arenga pinnata*). Sago starch from *M. sago* is the most commonly used and has been extensively studied by various researchers (Mohd Nurul, Mohd Azemi, & Manan, 1999; Ahmad, Williams, Doublier, Durand, & Buleon, 1999; Sopade & Kiaka, 2001; Maaruf, Che Man, Asbi, Junainah, & Kennedy, 2001; Aziz, 2002; Pei-Lang, Mohamed, & Karim, 2006; Singhal et al., 2008).

Another palm starch, obtained from *A. pinnata* or sugar palm is an economically important palm species in Indonesia. In Indonesia, sugar palm plantations cover 244.76 $km^2$ spread in 14 provinces (Effendi, 2010). Besides yielding sugar, sugar palm provides many useful products. Almost all parts of the plant are utilized (root, stem, fibers, leaves, sap from flowers, and fruit). Palm sugar produced from the nira sap of the inflorescence is the main product of *A. pinnata*. The sap is produced when the tree converts its starch into sugar to allow for the development of inflorescence. Arenga starch is usually processed when the tree is unproductive in terms of sugar and fruit. The production method is similar to that of sago starch and is often sold commercially under the same name. Wina, Evans, and Lowry (1986) reported that the starch content (fresh weight basis) of arenga ranged from 10.5% to 36.7% whereas that of sago ranged from 18.8% to 38.8%.

Sago starch has a multitude of uses in both food and non-food applications. In food processing, sago starch has been used as a stabilizer and thickener (Singhal et al., 2008). On the other hand, information about the characteristics of the physicochemical and functional properties, and application of arenga starch is still very limited. In West Java, several local wet noodle industries specifically prefer arenga starch to sago starch.

The choice of starch source for processing technology and starch-based product application depend on the functional properties of starches including thickening behavior and forming a gel or paste. The textural properties of the gelatinized and retrograded starches are important for their potential use in food systems and depend on the molecular component and structure of the starch (amylose and amylopectin). Amylose leads to higher viscosity values and more pronounced shear thinning behavior (Conola & Buleon, 2010). The presence of amylose in the continuous phase surrounding the swollen granules results in the formation of a strong gel on cooling (Liu, 2005). Waxy starch, which mainly consists of amylopectin, has a soft or sticky texture of gel or paste after gelatinization. The swelling ability also contributes to important characteristics of most starchy food products such as rheological behavior (Srichuwong, Sunarti, Mishima, Isono, & Hisamatsu, 2005b).

The aim of this research was to characterize the composition and physical properties of arenga starch in comparison to sago starch. Each type of starch was designed into two types of starch–water system, i.e. paste obtained from heated starch suspension at a low ratio of starch and gel from that at a high ratio.

* Corresponding author. Tel.: +81 29 838 8031; fax: +81 29 838 7996.
*E-mail addresses:* dede_adawiyah@yahoo.com, dede_adawiyah@ipb.ac.id (D.R. Adawiyah), tomokos@affrc.go.jp (T. Sasaki), kaoruk@affrc.go.jp (K. Kohyama).

0144-8617/$ – see front matter © 2012 Elsevier Ltd. All rights reserved.
http://dx.doi.org/10.1016/j.carbpol.2012.12.014

This information will provide useful insights into the potential applications of arenga and sago starches in the food industry, at both domestic and industrial scales.

## 2. Materials and methods

### 2.1. Materials

Arenga (*A. pinnata*) starch was obtained from an arenga starch processor in Sukabumi, whereas sago (*M. sago*) starch was obtained from Bogor, West Java, Indonesia. The starches were then further purified by washing, filtering, decantation, and drying.

### 2.2. Composition analysis

The standard AOAC method (Official methods of analysis, 1998) was used to measure moisture, ash, and protein (using a conversion factor of 6.25 from nitrogen content). Lipids were extracted with hexane using the Soxhlet method for 6 h. The samples were hydrolyzed with HCl before lipid extraction. Starch and amylose contents were analyzed by using commercial kits. The amyloglucosidase/α-amylase method K-TSTA (Megazyme International Ltd., Ireland) was used for the total starch assay, whereas a Megazyme kit for amylose/amylopectin assays K-AMYL was used to measure amylose content.

### 2.3. Differential scanning calorimetry (DSC)

Thermal properties were analyzed using an SSC5200H system with a DSC120 module (Seiko Instruments, Chiba, Japan) as described by Kohyama and Nishinari (1991) and Lu, Sasaki, Kobayashi, Li, and Kohyama (2009). Starches (approximately 10 mg) were weighed in a 70 μl silver pan. Distilled water was added with micro syringe to adjust moisture content to 70% (wet basis). The pan was sealed hermetically and allowed to stand for 24 h at room temperature before measurement (Yu & Christie, 2001). Another pan containing water (21.19 mg) was used as a reference. The sample and reference pans were heated at 1 °C/min from 30 °C to 130 °C. Melting points and enthalpies for indium and tin were used for calibration. The onset (*To*), peak (*Tp*) and conclusion (*Tc*) temperature were determined as illustrated in Fig. 1. The enthalpy of gelatinization ($\Delta H$) was calculated as the peak area of the endothermic curve and it was expressed in J/g dry starch. The DSC measurement were performed in five replications.

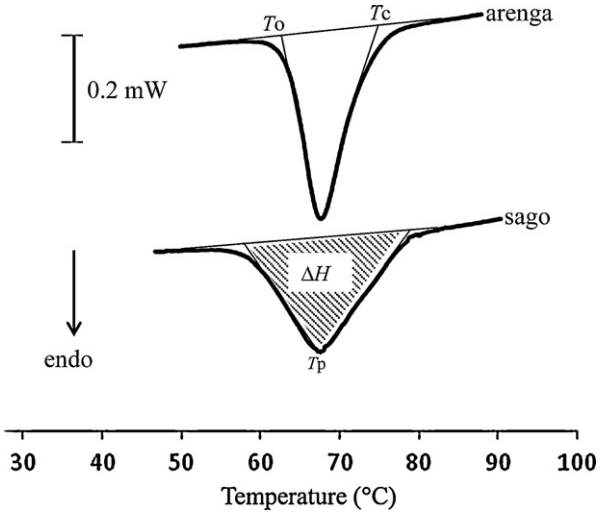


**Fig. 1.** DSC thermograms of sago and arenga starches. Starch concentration is 30% (w/w). Heating condition of DSC is from 30 °C to 130 °C at a constant rate of 1 °C/min; water as a reference. The DSC parameters are shown.

### 2.4. X-ray diffraction

The crystal structure and crystallinity of starch samples were studied using an X-ray diffractometer (Maxima XRD 7000, Shimadzu, Kyoto, Japan) with a copper anode X-ray tube at 40 kV and 30 mA. The monochromatic radiation wavelength was 0.154 nm. The starch sample was packed into 25 mm (dia) × 1 mm (d) aluminum sample holder for analysis. The scanning region of the diffraction angle ($2\theta$) was adjusted from 3° to 35°. The other operation condition were as follows: scanning rate at of 2°/min, step interval 0.02°, divergence and scatter slit 1° (Cheetam & Tao, 1998). Relative crystallinity (%) is defined as the peak area ratio of the crystalline component and was calculated using Rietveld analysis software developed by Shimadzu. Duplicate measurements were performed at ambient temperature (25 °C).

### 2.5. Swelling power

The swelling power of starches was measured according to Huang and Lai (2010) with some modification. Distilled water (1.5 ml) was added to 20 mg starch ($W_1$) in a 2.0 ml Eppendorf tube and mixed using a vortex mixer. The starch and water suspension were then heated in a water bath at 40 °C, 50 °C, 60 °C, 65 °C, 70 °C, 80 °C and 90 °C for 30 min. The tubes were mixed by inverting them twice every 5 min during the incubation period. The tubes were cooled at room temperature and then centrifuged at 13,000 × *g* for 10 min. The supernatant was separated from sediment and dried to constant weight ($W_2$) at 130 °C for 2 h. The sediment was weighed ($W_3$). The water soluble index (WSI) and swelling power (SP) were calculated according to Li and Yeh (2001) and the data were reported as averages of three replications.

$$\text{WSI}(\%) = \frac{W_2}{W_1} \times 100$$

$$\text{SP}(g/g) = \frac{W_3}{W_1}(100 - \text{WSI})$$

### 2.6. Rheological properties

Rheological properties were measured using a stress-controlled rheometer (AR-G2, TA Instruments, New Castle, USA).

### 2.7. Viscometric flow

Viscosity was measured for 2% (w/v) and 3% (w/v) of starch paste system. Starch paste was prepared by weighing starch and adding water followed by gently stirring for 15 min at room temperature and continuously heated and stirred at 80–85 °C for another 15 min. The measurement was conducted in a continuous flow test using a cone and plate geometry with a cone angle of 0°58′51″ and a diameter of 40 mm at 25 °C after the samples had been cooled to room temperature (25 °C). The shear rate range was set from 0.01 to 10,000 $s^{-1}$, and measurement time was 2 min. Viscometric flow measurement was performed in three replications.

### 2.8. Viscoelastic properties

Dynamic viscoelastic properties were measured in frequency sweep and oscillatory stress sweep tests. The frequency sweep test was conducted to determine transition from sol (liquid state) to gel (solid-like) at low starch concentrations of starch paste from 1% (w/v) to 3% (w/v). Starch paste preparation and cone geometry were the same as viscometric flow measurement. The frequency range was raised from 0.01 to 100 Hz at a constant temperature of 25 °C and constant oscillatory stress in linear region (1 Pa). Linear

viscoelastic region was determined when viscoelastic moduli ($G'$ and $G''$) were constant or plateau region during oscilation stress.

Oscillatory stress sweep tests were conducted for starch paste [2–6% (w/v) concentration of starches] and starch gel [10% (w/v) and 20% (w/v) concentration of starches]. Preparation of starch paste [2–6% (w/v) of starches] was the same as for viscometric flow test. For gel preparation, 10% (w/v) and 20% (w/v) starch suspensins were gently stirred for 15 min at room temperature, and heated at 80–85 °C for 30 min. The hot starch paste were poured between two glass plates with a spacer of 2 mm and cooled at room temperature for 2 h to form gel. The oscillatory stress for the starch paste sample was set from 1 to 100 Pa at a constant temperature of 25 °C and constant frequency of 1 Hz using a 40 mm parallel plate geometry; the gap was set at 1000 μm for paste or as gel thickness. The oscillatory sweep test for starch gel was conducted using 20 mm plate geometry from 1 to 10,000 Pa at a constant temperature of 25 °C and constant frequency of 1 Hz. The values of the storage modulus ($G'$, Pa), loss modulus ($G''$, Pa), and tan delta ($\tan\delta = G''/G'$) were calculated.

### 2.9. Texture analysis

Starch gels were subjected to texture analysis. A 10% (w/v, dry basis) of starch suspension was stirred at room temperature for 15 min followed by continuous heating at 80 °C for 30 min. The samples were poured into plastic cylinders (diameter of 23 mm and height of approximately 15 mm), and cooled to room temperature. The gels were stored in a refrigerator at 10 °C overnight, and then stored at room temperature for 1 h before measurements were performed. The duplicate preparation of five specimens were tested for each sample.

Textural properties were measured using a Texture Analyzer (TA-XT plus, Stable Microsystems, Godalming, UK) equipped with a load cell of 50 N. Two types of compression tests, a uniaxial compression test and texture profile analysis (TPA), were performed using a compression plate with a diameter of 100 mm (P/100).

In the uniaxial compression test, starch gel was compressed at a constant speed of 1 mm/s until the strain reached 90% of its original thickness. The pre-test and post-test speeds were 2 mm/s and the trigger force was at 0.01 N. The mechanical stress (Pa) was calculated as the force divided by the initial cross sectional area (415 $mm^2$) of the sample, and strain (%) was defined as the ratio of deformation to initial height. The work was calculated as the area under force–distance curve (N mm). The shoulder point was defined as the peak of the first derivative of force–strain curve (see Fig. 2 insets). The breaking point was determined by the first reduction of force or first peak in the force–strain curve. The stress, strain and work at the shoulder, and breaking points and stress value at each 10% strain up to the shoulder point were extracted. The force values at 70% and higher strains, and work until 90% strain were also measured to characterize the texture of sample gels after broken. The adhesive force (N) was defined as the maximum negative force measured while the plate was pulled away from the sample. The breaking point, shoulder point, and adhesive force are illustrated in Fig. 2.

For TPA (texture profile analysis) experiment, the starch gels were compressed twice at a test speed of 1 mm/s until 50% strain. A deformation level of 50% was applied after a preliminary test to determine the maximum strain level before destruction of the starch gels. Originally, the samples were usually subjected to large deformation (75–80%) in TPA experiments. However, Pons and Fiszman (1996) recommended using a deformation level between 20% and 50% in starch gel food system, because under large deformation, the samples collapsed and invalid parameters were obtained. A small deformation level (25%) during TPA testing of starch gels was also applied by Huang, Kennedy, Li, Xu, and Xie (2007) and Teng, Chin, and Yusof (2011) to avoid total destruction of the gel structure during the first compression. On the basis of the breaking strain information from the uniaxial compression test, 50% strain was applied in our experiment.

The time interval between compression cycles was 10 s, post-test speed was 5 mm/s and the trigger was 0.01 N. TPA parameters were determined according to Bourne (2002). Hardness (N) was defined as the maximum force measured during the first compression. Cohesiveness was measured as the work, which is the area under the force–distance curve during the second compression divided by the work during the first compression. Adhesiveness was defined as the negative force area after the first simulated bite

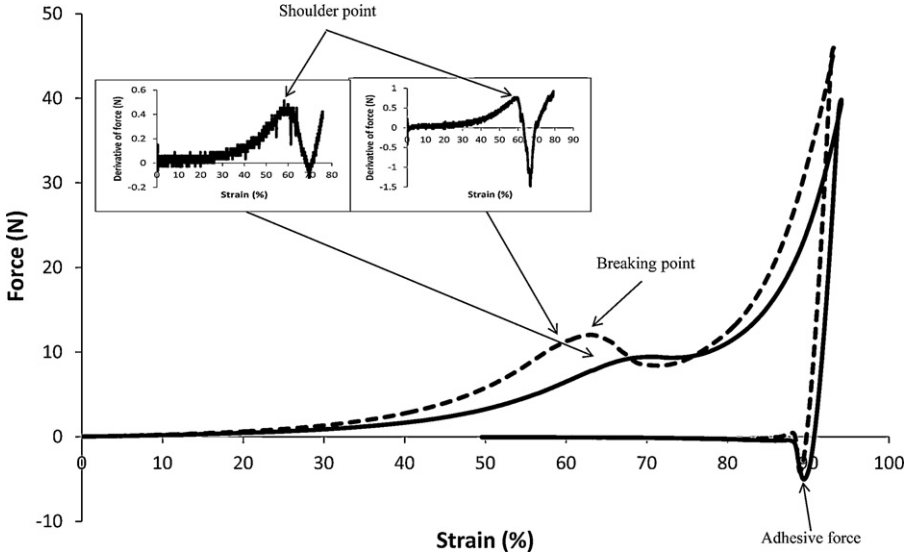


**Fig. 2.** Uniaxial compression curves for 10% (w/v) arenga (- - -) and sago (—) starch gels. Gels are compressed at 25 °C and 1 mm/s until 90% strain. Some specific points of the curves are shown and the definition of the adhesive force is shown. The insets are the first derivative of force versus strain, which was used to determine the strain value at the shoulder point.

**Table 1**
Composition of arenga and sago starches.

| Component | Arenga | Sago | $p$ ($t$-test)[a] |
|---|---|---|---|
| Moisture (% w/w) | 9.03 ± 0.00 | 9.17 ± 0.00 | 0.690 |
| Ash (% w/w) | 0.20 ± 0.00 | 0.16 ± 0.00 | 0.032 |
| Protein (% w/w) | 0.10 ± 0.00 | 0.08 ± 0.00 | 0.023 |
| Fat (% w/w) | 0.27 ± 0.00 | 0.24 ± 0.00 | 0.014 |
| Starch (% w/w) | 86.8 ± 1.74 | 87.6 ± 2.50 | 0.487 |
| Amylose (% w/w starch) | 36.6 ± 1.55 | 37.0 ± 1.46 | 0.707 |

Mean and standard deviation of two or three replicates.
[a] Probability value from $t$-statistic test.

represented by the work necessary to pull the plate away from the sample.

### 2.10. Statistical analysis

Statistical analysis was conducted using $t$-test (two tails) for two samples of unequal variance (Microsoft Excel). The probability values for no-difference between sago and arenga samples are presented as $p$($t$-test).

## 3. Results and discussion

### 3.1. Composition of arenga and sago starches

The composition of arenga and sago starches is presented in Table 1. Both starches have very low protein contents of 0.10% (w/w) and 0.08% (w/w) for arenga and sago starch, respectively. Fat contents of both starches were also low at 0.27% (w/w) and 0.24% (w/w), respectively. Ahmad et al. (1999) reported crude protein in sago starch varied from 0.13% (w/w) to 0.25% (w/w), whereas crude fat content varied from 0.10% (w/w) to 0.2% (w/w). The quantities of starch in arenga and sago were 92.7% (w/w) and 93.8% (w/w) dry weight, respectively. The amylose content of sago starch was 36.6% (w/w), whereas arenga starch had an amylose content of 37.0% (w/w). The amylose content of the two types of Indonesian palm starch derived from different genera (*Metroxyllon* and *Arenga*) were not significantly different ($p > 0.05$).

### 3.2. Gelatinization properties

Gelatinization characteristics of arenga and sago starch were measured by DSC as $To$, $Tp$, $Tc$ and $\Delta H$ (Table 2 and Fig. 1). There were significant differences in gelatinization characteristics between arenga and sago starch. The $Tp$ values for arenga and sago starches were detected at approximately the same value of 67 °C, although the $Tp$ of arenga starch was statistically significantly higher ($p < 0.001$). Ahmad et al. (1999) and Maaruf et al. (2001) reported that $Tp$ of sago starch measured using DSC was approximately 70 °C.

In general, the endothermic curve of sago starch was wider than arenga starch and the melting temperature range ($Tc - To$) of sago starch was significantly larger than that of arenga starch,

**Table 2**
Gelatinization characteristics of arenga and sago starches of 30% (w/w).

| Gelatinization parameters | Arenga | Sago | $p$ ($t$-test)[a] |
|---|---|---|---|
| $T0$ (°C) | 63.0 ± 0.12 | 58.1 ± 0.28 | 0.000 |
| $Tp$ (°C) | 67.7 ± 0.07 | 67.3 ± 0.21 | 0.017 |
| $Tc$ (°C) | 74.6 ± 0.42 | 79.4 ± 0.88 | 0.000 |
| Range ($Tc - To$) (°C) | 11.6 ± 0.49 | 21.3 ± 0.79 | 0.000 |
| $\Delta H$ (J/g) | 15.4 ± 0.25 | 16.4 ± 0.24 | 0.001 |

Heating rate of 1 °C/min.
Mean and standard deviation of five replicates.
[a] Probability value from $t$-statistic test.

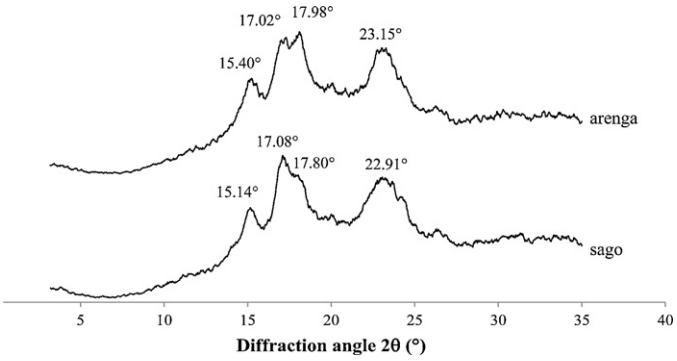


**Fig. 3.** X-ray diffraction pattern for arenga and sago starches. Moisture contents are 9.03% (w/w, db) for arenga and 9.17% (w/w, db) for sago, respectively.

as is clearly shown in Fig. 1. The $\Delta H$ of arenga starch was significantly smaller than that of sago starch, although both starches have similar amylose contents. This result could be caused by the difference in amylopectin crystalline structure. The $\Delta H$ primarily reflects the loss of molecular (double-helical) order (Cooke & Gidley, 1992). Tester and Morrison (1990a) postulated that the DSC gelatinization endotherm gives a measure of the crystalline quality (effectively double helix length) from $Tp$ and overall crystallinity (quality × quantity) from $\Delta H$. Gelatinization behavior measured by DSC was reported to be highly dependent on the amylopectin unit-chain length distribution in rice starch (Vandaputte, Derycke, Geeroms, & Delcour, 2003a) and starches from different botanical sources (Srichuwong, Sunarti, Mishima, Isono, & Hisamatsu, 2005a).

### 3.3. X-ray diffraction

The X-ray diffraction of arenga and sago starches (Fig. 3) showed similar C-type patterns. Both starches showed four strong peaks at $2\theta$ values of around 15°, 17°, 18°, and 23°. The crystalline structure of sago starch has already been reported to be C-type (a mixture of A- and B-type diffraction) (Ahmad et al., 1999; Pukkahuta & Varavinit, 2007; Karim et al., 2008). Karim et al. (2008) reported that the native sago starch showed strong peak at $2\theta$ of 15.3°, 17.3°, 18.3°, and 23.5°. The relative crystallinity of arenga starch (23.5%) was significantly lower ($p < 0.05$) than that of sago (27.5%). The crystallinity values correlated well with $\Delta H$ from the DSC experiments mentioned above. The $\Delta H$ of arenga and sago starches were 15.4 J/g and 16.4 J/g, respectively.

### 3.4. Swelling power

The temperature dependence of the swelling power and solubility index are shown in Fig. 4. The swelling power increased significantly when heating temperature was 70 °C. The same result for sago starch was reported by Srichuwong et al. (2005b) who showed that swelling power showed increased significantly at 70 °C. This could be associated with the gelatinization properties of both starches. Arenga and sago starches have similar $Tp$ values of approximately 67 °C. Li and Yeh (2001) found that swelling power correlated well with ratio of heating temperature ($T$) to $Tp$ or $T/Tp$ for various starches and $Tp$ was a good reference point for considering temperature effects.

The swelling capacity of sago starch was higher than that of arenga starch. It is related to $\Delta H$, where the $\Delta H$ of sago starch was significantly greater than that of arenga starch as mentioned above. Sasaki and Matsuki (1998) found a positive correlation between swelling power and enthalpy. Tester and Morrison (1990b) suggested that maximum swelling factor (swollen volume/initial

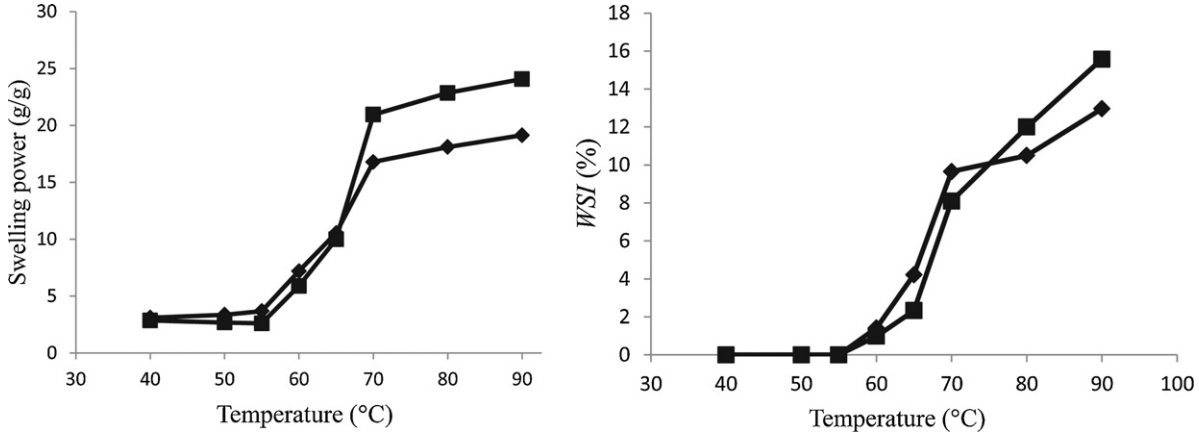


**Fig. 4.** Swelling power and water soluble index (WSI) of arenga (♦) and sago starches (■). Starch (20 mg) is dispersed in 1.5 ml of water and heated from 40 °C to 90 °C for 30 min.

volume) may be related to the molecular weight and shape of the whole amylopectin molecule. Vandaputte, Derycke, Geeroms, and Delcour (2003b) and Srichuwong et al. (2005b) also reported that swelling power was affected by the structural aspect of amylopectin.

The temperature dependency of the water solubility index (WSI) and that of the swelling power were consistent. Upon increasing the temperature in the presence of water, the mobility of the starch molecules increases, weakening the binding forces; thus, a parallel effect is obtained in both the swelling capacity (water diffusion into the starch granules) and solubility (Lawal et al., 2011).

### 3.5. Rheological properties

The viscometric flow test of 2% (w/v) and 3% (w/v) arenga and sago starch pastes showed shear thinning behavior where viscosity decreased with an increase in shear rate (Fig. 5). Conola and Buleon (2010) stated that at low concentration of starch (<10%, w/w) pastes from starch exhibit shear thinning with thixotropic behavior. The viscosity of starch suspension is strongly influenced by the swelling of starch granules (Liu, 2005). Sago starch paste was considerably more viscous than arenga starch. The swelling power of sago starch was higher than that of arenga starch as mentioned above, which suggests that the higher swelling power of sago starch granules contribute to the higher viscosity of its paste. The loss of free water

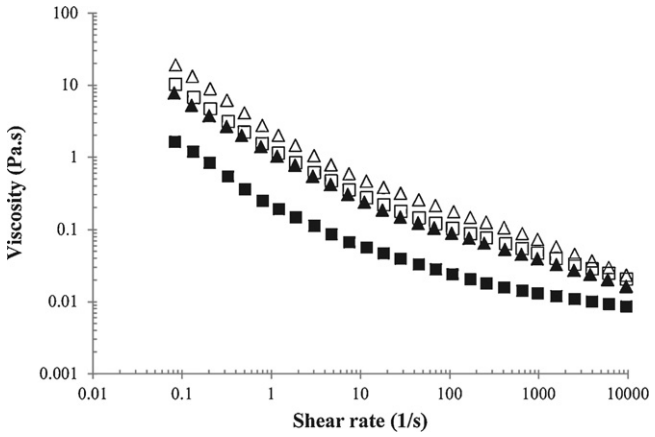


**Fig. 5.** Viscosity profile of arenga and sago starch pastes. The shear rate is raised from 0.01 to 10,000 $s^{-1}$ for 2 min at 25 °C. The concentration of arenga starch paste was 2% (■) and 3% (□) and sago starch paste was 2% (▲) and 3% (△).

and restriction of water flow, due to enormously swollen granules occupying more space, contribute to the increased viscosity of the starch system (Srichuwong et al., 2005b).

A frequency sweep test was performed to determine the sol–gel transition concentration of starch paste. The sol–gel transition is a state change from sol or liquid state where loss modulus, $G''$, is dominated to the gel or solid state where storage modulus, $G'$, is dominated. Fig. 6 shows the differences between sol and gel characteristics of two concentrations of arenga and sago starch pastes. Sol characteristics were shown by 2.1% (w/v) arenga and 1.6% (w/v) sago starch pastes, which exhibited a significant dependency of $G'$ and $G''$ on frequency; $G'$ was smaller than $G''$ for the lower frequency range (<10 rad/s). Gel characteristics were shown by 2.4% (w/v) arenga and 1.8% sago starch pastes, which showed lower dependency of $G'$ and $G''$ on frequency and $G'$ is always higher than $G''$. A gel can be defined as an intermediate state between a liquid and solid like rheological behavior. A gel should exhibit a solid-like mechanical spectrum (that is, $G' > G''$) throughout the experimentally accessible frequency range and little frequency dependence of the moduli (Ikeda & Nishinari, 2001; Nishinari, 2009).

Fig. 7 shows changes in $\tan\delta$ during the frequency sweep for arenga and sago starch pastes. The $\tan\delta$ in frequency sweep tests was independent at concentrations of 1.8% (w/v) for sago and 2.4% (w/v) for arenga starch pastes. The dependency of $G'$, $G''$ and $\tan\delta$ on the frequency sweeps in Figs. 6 and 7 clearly showed that sago starch can form gel or solid-like state at a lower concentration than arenga starch. Therefore, sago starch is more suitable as a thickener because lesser quantity will be required to obtain a paste (thick solution) as compare with arenga starch, which was also shown by the viscometric flow (Fig. 5).

Fig. 8 shows the storage modulus ($G'$) and loss modulus ($G''$) of arenga and sago starch pastes at concentration 2–6% (w/v) and starch gels at 10% and 20% (w/v) derived from oscillation sweep test. At low concentrations 2–4% (w/v), $G'$ and $G''$ of arenga starch paste were lower than that of sago. Arenga and sago starch pastes would have the same storage modulus at concentrations of approximately 4.5% (w/v). Above this point, the $G'$ and $G''$ values of arenga starch increase more significantly than that of sago starch. An increase of $G'$ indicates increasing rigidity of the sample associated with the capability to form of the elastic gel structure after cooling. At high concentrations of starch (10% and 20%, w/v) in the gel form, arenga starch was more rigid gel with a higher elasticity modulus than sago starch.

The data from Fig. 8 provide valuable information for the different applications of arenga and sago starches. The low concentration experiment results strengthen the conclusion, from viscometric

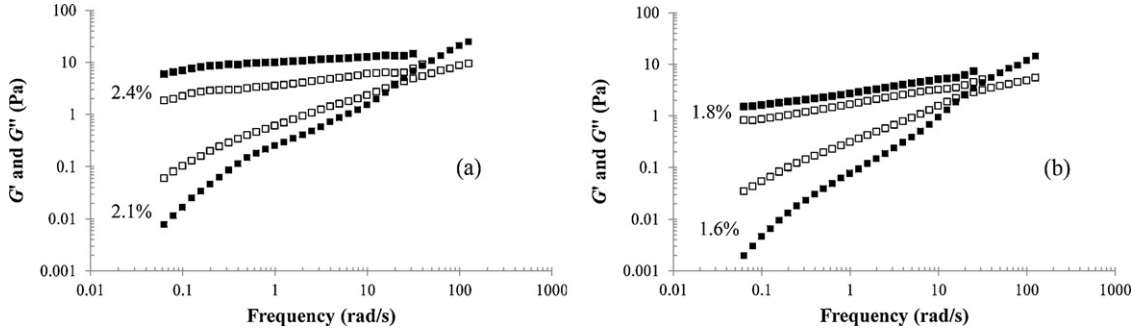


**Fig. 6.** Frequency dependence of storage $G'$ (■) and loss $G''$ (□) moduli of arenga (a) and sago (b) starch pastes. Frequency is raised from 0.01 to 100 Hz under a constant oscillatory stress of 1 Pa at 25 °C. The sol characteristics are shown for the concentration, in % (w/v), of arenga (2.1) and sago (1.6), whereas the gel characteristics are shown for arenga (2.4) and sago (1.8).

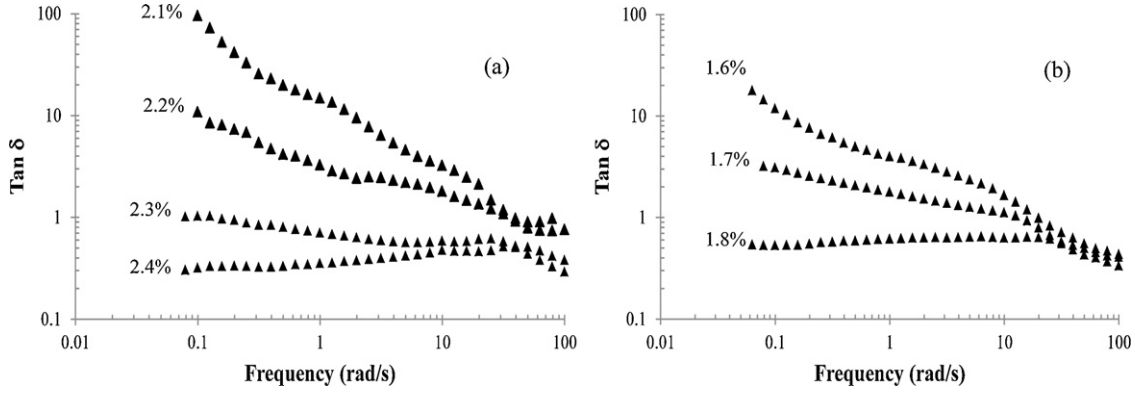


**Fig. 7.** Frequency dependence of tan $\delta$ of arenga (a) and sago (b) starch pastes. Test conditions are the same as in Fig. 6. The sol characteristics are shown for the concentration, in % (w/v), of arenga (2.1, 2.2 and 2.3) and sago (1.6 and 1.7). The gel characteristics are shown for arenga (2.4) and sago (1.8).

flow and frequency sweep tests, that sago starch will produce a more viscous and elastic solution than arenga starch. As a thickener, sago starch is better than arenga starch. However, at high concentration (above 5%), arenga starch will produce a more rigid and elastic solid-gel than sago starch.

The differences in rheological properties between arenga and sago starches are mainly caused by the differences in the swelling power capacity that is related to crystalline quality of amylopectin ($\Delta H$, $Tc - To$ and relative crystalinity). The structure of amylopectin plays a critical role in the differences of rheological properties between arenga and sago starches because there was no significant difference in amylose and amylopectin ratio between two starches. The structural aspects of amylopectin need to be further evaluated, such as amylopectin chain length distribution.

### 3.6. Textural properties

The simple compression curve derived from uniaxial compression test of 10% (w/v) arenga and sago starch gels is presented in Fig. 2. Arenga starch gel exhibited a clear breaking point that was determined as a maximum point of first peak, and it was detected at 60.1% of strain. The corresponding points could not be determined for sago starch gel. The shoulder point, the strain was defined as the peak in the first derivative of compression force was derived as

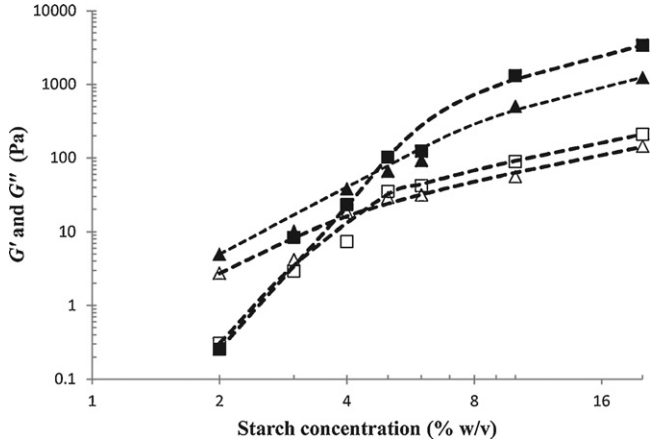


**Fig. 8.** Storage ($G'$) and loss ($G''$) moduli of sago and arenga starch pastes at 2–20% (w/v) concentrations from oscillation stress sweep (1–10,000 Pa) at 25 °C and 1 Hz. (■) $G'$ of arenga; (□) $G''$ of arenga; (▲) $G'$ of sago; (△) $G''$ of sago.

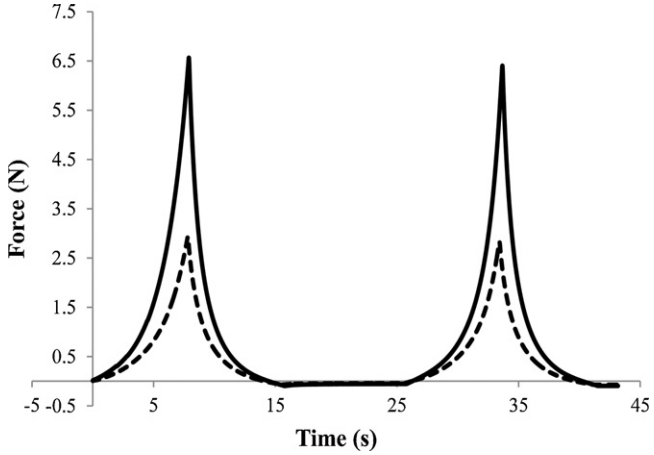


**Fig. 9.** Texture profile analysis (TPA) curves of 10% (w/v) arenga (- - -) and sago (—) starch gels at 25 °C and 1 mm/s until 50% of strain.

**Table 3**
Mechanical properties of 10% (w/v) arenga and sago starch gels from uniaxial compression test at 25 °C and 1 mm/s until 90% of strain.

| Mechanical parameters | Arenga | Sago | $p$ ($t$-test)[b] |
|---|---|---|---|
| Stress at 10% strain (kPa) | 0.61 ± 0.10 | 0.41 ± 0.04 | 0.000 |
| Stress at shoulder point (kPa) | 23.0 ± 3.65 | 15.5 ± 0.96 | 0.000 |
| Strain at shoulder point (%) | 54.4 ± 3.54 | 59.1 ± 2.28 | 0.003 |
| Work until shoulder point (N mm) | 20.2 ± 1.80 | 14.1 ± 0.82 | 0.000 |
| Breaking stress (kPa) | 29.8 ± 2.64 | nd[a] | – |
| Breaking strain (%) | 60.1 ± 2.61 | nd[a] | – |
| Work until breaking point (N mm) | 29.6 ± 2.45 | nd[a] | – |
| Compressive force after breaking at 70% strain (N) | 8.77 ± 0.59 | 9.97 ± 1.11 | 0.032 |
| Compressive force at 90% strain (N) | 43.8 ± 2.34 | 44.0 ± 3.89 | 0.869 |
| Work until 90% strain (N mm) | 108 ± 6.11 | 90.3 ± 8.37 | 0.000 |
| Adhesive force (N) | −3.64 ± 0.96 | −8.99 ± 1.57 | 0.000 |

Mean and standard deviation of five replicates.
[a] Not detected.
[b] Probability value from $t$-statistic test.

a common specific point. Sago starch gel did not show a maximum point in the compression force curve; however, its deformation could be seen as a shoulder-shaped change in the compression curve and the peak from first derivative of compression curve. The shoulder point of sago starch gel was detected at 59.1% strain, that was below the breaking point, whereas that of arenga starch gel was found at 54.4% strain (Table 3).

Table 3 shows the mechanical properties of arenga and sago starch gel derived from the uniaxial compression (force–strain) curve. The stress value at 10% strain for arenga starch gel was significantly greater than that for sago starch ($p < 0.05$) and similar results were found at any strain level below the shoulder point (data not shown). This fact is consistent with the rheological data showing that elastic modulus ($G'$) of 10% (w/v) arenga starch gel was higher than that of sago starch. After the gels were broken or fractured, there were no significant differences in compression force at 60–90% strain between arenga and sago starch gel ($p > 0.05$). The overall work or compression energy until 90% strain, arenga starch gel was significantly higher than that of sago starch.

The mechanical properties measurements were conducted to determine the resistance of starch gels to intense stress during processing. For example, starch was gelatinized, mixed and stirred with un-gelatinized starch to form non-sticky dough during starch noodle processing. The dough was then extruded through the holes to form noodles (Tan, Li, & Tan, 2009). Arenga starch gel had a higher resistance during processing to form a gel food or dough because the work or energy to deform starch gel was significantly higher in arenga starch gels which were also less adhesive than that in sago starch. The work value until the shoulder point of arenga starch gel was 20.2 N mm, while that of sago starch was 14.1 N mm. Those different properties may be the reason why arenga starch has been preferred to sago starch for making noodles, in the area of West Java in Indonesia.

The TPA (texture profile analysis) was conducted (Fig. 9) to describe the procedure of compressing bite-size pieces of food using a mechanical device, and to analyze the force–time curve resulting from simulated mastication (Bourne, 2002). The TPA parameters showed that hardness was the main textural property difference between arenga and sago starch gels (Table 4). The hardness of arenga starch gel was significantly higher than sago starch ($p < 0.001$). The cohesiveness value for gels of both starches were similar (0.85 and 0.87). Cohesiveness indicates how the sample retains its structure after the first compression (Teng et al., 2011).

The adhesive properties of arenga and sago starch gels obtained from uniaxial compression test and TPA test differed. Adhesive force in the single compression test was calculated after a large deformation (90% strain) to mimic chewing conditions (Kohyama, Hanyu, Hayakawa, & Sasaki, 2010), whereas adhesiveness in the TPA test, to evaluate gels before breaking point (50% strain), indicates difficulty in handling before gels are eaten. As there was no breakdown of either of the starch gels at up to 50% strain, the adhesiveness and cohesiveness of both starches could be compared. The adhesiveness of arenga starch gel was slightly higher than that of sago starch under small deformation, however, following breakdown the arenga starch gel was less adhesive than sago starch. These observations suggest that arenga starch can make a firmer and more adhesive gel than sago at the same concentration. Therefore, an appropriate gel for the desired use can be made with a lower concentration of arenga starch, and arenga starch would produce a less adhesive gel in the mouth than sago. Sensory properties of these gels need to be further evaluated for the practicality.

**Table 4**
Texture profiles analysis (TPA) of 10% (w/v) arenga and sago starch gels at 25 °C and 1 mm/s until 50% strain.

| TPA parameter | Arenga | Sago | $p$ ($t$-test)[a] |
|---|---|---|---|
| Hardness (N) | 7.02 ± 0.51 | 3.05 ± 0.31 | 0.000 |
| Cohesiveness | 0.85 ± 0.02 | 0.87 ± 0.02 | 0.024 |
| Adhesiveness (N s) | −0.77 ± 0.14 | −0.53 ± 0.12 | 0.003 |

Mean and standard deviation of five replicates.
[a] Probability value from $t$-statistic test.

## 4. Conclusions

The two different types of palm starches (*Arenga pinnata* and *Metroxylon sago*) did not show significant differences in their chemical compositions, total amylose contents and peak gelatinization temperatures (*T*p). However, rheological properties, including viscosity of starch paste and viscoelastic behavior of starch paste and gel, and textural properties of starch gel especially in breaking pattern, adhesiveness and hardness, of both starches differed significantly. Variations in the rheological properties and textural properties between arenga and sago starch pastes and gels were caused by significant differences in their swelling power, related to the amylopectin crystalline qualities, measured as $\Delta H$, $Tc - To$ and relative crystallinity. Considering the rheological and textural properties, sago starch is more suitable for use as a thickener because it produces a more viscous, thicker solution at a low concentration than arenga starch. However, arenga starch is more appropriate for producing starch gels or starch doughs than sago starch because it forms a firmer, more resistant gel at concentrations above the gel point.

## Acknowledgement

The authors gratefully acknowledge the Kirin Holding Co. Japan and United Nation University (UNU) for awarding research fellowship program at NFRI-NARO-Japan.

## References

Ahmad, F. B., Williams, P. A., Doublier, J. L., Durand, S., & Buleon, A. (1999). Physico-chemical characterization of sago starch. *Carbohydrate Polymers*, *38*, 361–370.
AOAC, Association of Official Analytical Chemists. (1998). *Official methods of analysis* (16th ed.). Washington, DC: AOAC.
Aziz, S. A. (2002). Sago starch and its utilization. *Journal of Bioscience and Bioengineering*, *94*, 526–529.
Bourne, M. C. (2002). Food texture and viscosity: Concept and measurement. New York: Academic Press, [Chapter 4].
Cheetam, N. W. H., & Tao, L. (1998). Variation in crystalline type amylose content in maize starch granules: An X ray powder diffraction study. *Carbohydrate Polymers*, *26*, 277–284.

Conola, P., & Buleon, A. (2010). Thermal transition of starches. In A. C. Bertolini (Ed.), *Starches: Characterization, properties and applications* (pp. 71–102). Boca Rotan: CRC press.

Cooke, F., & Gidley, M. J. (1992). Loss of crystalline and molecular order during starch gelatinization: Origin of enthalphic transition. *Carbohydrate Research*, *227*, 102–112.

Effendi, D. S. (2010). Prospek pengembangan tanaman aren (*Arenga pinnata* Merr) mendukung kebutuhan bioetanol di Indonesia. *Perspektif*, *9*, 36–46.

Huang, M., Kennedy, J. F., Li, B., Xu, X., & Xie, B. J. (2007). Characters of rice starch gel modified by gellan, carrageenan, and glucomannan: A texture profile analysis study. *Carbohydrate Polymers*, *69*, 411–418.

Huang, Y. C., & Lai, H. M. (2010). Noodle quality affected by different cereal starches. *Journal of Food Engineering*, *97*, 135–142.

Ikeda, S., & Nishinari, K. (2001). Weak gel-type rheological properties of aqueous dispersions of nonaggregated κ-carrageenan helices. *Journal of Agricultural and Food Chemistry*, *49*, 4436–4441.

Karim, A. A., Nadiha, M. Z., Chen, F. K., Phuah, Y. P., Chui, Y. M., & Fazilah, A. (2008). Pasting and retrogradation properties of alkali-treated sago (*Metroxylon sagu*) starch. *Food Hydrocolloids*, *22*, 1044–1053.

Kohyama, K., & Nishinari, K. (1991). Effect of soluble sugars on gelatinization and retrogradation of sweet potato starch. *Journal of Agricultural and Food Chemistry*, *39*, 1406–1410.

Kohyama, K., Hanyu, T., Hayakawa, F., & Sasaki, T. (2010). Electromyographic measurement of eating behavior for buckwheat noodles. *Bioscience, Biotechnology and Biochemistry*, *74*, 56–62.

Lawal, O. S., Lapasin, R., Bellich, B., Olayiwola, T. O., Cesaro, A., Yoshimura, M., et al. (2011). Rheology and functional properties of starches isolated from five improved rice varieties from West Africa. *Food Hydrocolloids*, *25*, 1785–1792.

Li, J. Y., & Yeh, A. I. (2001). Relationship between thermal, rheological characteristics and swelling power for various starches. *Journal of Food Engineering*, *50*, 141–148.

Liu, Q. (2005). Understanding starches and their role. In S. W. Cui (Ed.), *Food carbohydrates* (pp. 309–349). Boca Raton: Taylor & Francis.

Lu, Z. H., Sasaki, T., Kobayashi, N., Li, L. T., & Kohyama, K. (2009). Elucidation of fermentation effect of rice noodles using combined dynamic viscoelasticity and thermal analyses. *Cereal Chemistry*, *86*, 70–75.

Maaruf, A. G., Che Man, Y. B., Asbi, B. A., Junainah, A. H., & Kennedy, J. F. (2001). Effect of water content on the gelatinisation temperature of sago starch. *Carbohydrate Polymers*, *46*, 331–337.

Mohd Nurul, I., Mohd Azemi, B. M. N., & Manan, D. M. A. (1999). Rheological behavior of sago (*Metroxylon sagu*) starch paste. *Food Chemistry*, *64*, 501–505.

Nishinari, K. (2009). Some thought on the definition of gel. *Progress of Colloid Polymer Science*, *136*, 87–94.

Pei-Lang, A. T., Mohamed, A. M. D., & Karim, A. A. (2006). Sago starch and composition of associated components in palms of different growth stages. *Carbohydrate Polymers*, *63*, 283–286.

Pukkahuta, C., & Varavinit, S. (2007). Structural transformation of sago starch by heat moisture treatment and osmotic-pressure treatment. *Starch/Starke*, *59*, 624–631.

Pons, M., & Fiszman, S. M. (1996). Instrumental texture profile analysis with particular reference to gelled systems. *Journal of Texture Studies*, *27*, 597–624.

Sasaki, T., & Matsuki, J. (1998). Effect of wheat starch structure on swelling power. *Cereal Chemistry*, *75*, 525–529.

Singhal, R. S., Kennedy, J. F., Gopalakrishnan, S. M., Kaczmarek, A., Knill, C. J., & Akmar, P. F. (2008). Industrial production, processing and utilization of sago palm-derived products. *Carbohydrate Polymers*, *72*, 1–20.

Sopade, P. A., & Kiaka, K. (2001). Rheology and microstructure of sago starch from Papua New Guinea. *Journal of Food Engineering*, *50*, 47–57.

Srichuwong, S., Sunarti, T. C., Mishima, T., Isono, N., & Hisamatsu, M. (2005a). Starches from different botanical sources I: Contribution of amylopectin fine structure to thermal properties and enzyme digestibility. *Carbohydrate Polymers*, *60*, 529–538.

Srichuwong, S., Sunarti, T. C., Mishima, T., Isono, N., & Hisamatsu, M. (2005b). Starches from different botanical sources II: Contribution of starch structure to swelling and pasting properties. *Carbohydrate Polymers*, *62*, 25–34.

Tan, O. Z., Li, O. Z., & Tan, B. (2009). Starch noodles: History, classification, materials, processing, structure, nutrition quality evaluating and improving. *Food Research International*, *42*, 551–576.

Teng, L. Y., Chin, N. L., & Yusof, Y. A. (2011). Rheological and textural studies of fresh and freeze–thawed native sago starch–sugar gels I. Optimisation using response surface methodology. *Food Hydrocolloids*, *25*, 1530–1537.

Tester, R. F., & Morrison, W. R. (1990a). Swelling and gelatinization of cereal starches. I. Effect of amylopectin amylose and lipids. *Cereal Chemistry*, *67*, 551–557.

Tester, R. F., & Morrison, W. R. (1990b). Swelling and gelatinization of cereal starches. II. Waxy rice starches. *Cereal Chemistry*, *67*, 558–563.

Yu, L., & Christie, G. (2001). Measurement of starch thermal transition using differential scanning calorimetry. *Carbohydrate Polymers*, *46*, 179–184.

Vandaputte, G. E., Derycke, V., Geeroms, J., & Delcour, J. A. (2003a). Rice starches. I. Structural aspects provide insight into crystallinity characteristics and gelatinization behavior of granular starch. *Journal of Cereal Science*, *38*, 43–52.

Vandaputte, G. E., Derycke, V., Geeroms, J., & Delcour, J. A. (2003b). Rice starches. II. Structural aspects provide insight into swelling and pasting properties. *Journal of Cereal Science*, *38*, 53–59.

Wina, E., Evans, A. J., & Lowry, J. B. (1986). The composition of pith from sago palms *Metroxylon sago* and *Arenga pinnata*. *Journal of The Science of Food and Agriculture*, *37*, 352–358.